Article:
Borissova, A orcid.org/0000-0003-3169-1118 (2019) Driving Force of Crystallization Based on Diffusion in the Boundary and the Integration Layers. Chemical Engineering and Technology, 42 (3). pp. 661-668. ISSN 0930-7516

https://doi.org/10.1002/ceat.201800255

Driving force of crystallisation based on diffusion in the boundary and the integration layers

Antonia Borissova[1]*
[1]School of Chemical and Process Engineering, University of Leeds, Leeds, LS2 9JT, UK
*Correspondence: Antonia Borissova (E-mail: A.Borissova@leeds.ac.uk), School of Chemical and Process Engineering, University of Leeds, Leeds, LS2 9JT, UK

Abstract:

Crystal growth rates are notoriously difficult to predict and even experimental data are often inconsistent. By allowing for mass and energy diffusion through the molecular and thermal layers surrounding a growing crystal and for the heat effect of crystallization, a new model of crystal growth from solution is proposed and applied to crystallization of potassium chloride from aqueous solution. The driving force for crystal growth was calculated using the solubility at the interface temperature in contrast to the conventional one based on bulk temperature. A positive heat effect at the crystal interface as well as the resistances to the mass and energy transfer processes to and from the crystal surface can reduce the conventional driving force for crystal growth by more than 20%.

Keywords: Boundary layer, Crystal growth rate, Driving force, Integration (Desolvation) layer, Mathematical modelling

1. Introduction

Crystal growth is a complex process and is frequently modelled using empirical correlations which do not accurately represent the true physical phenomena. The crystal growth power constant is referred to as the order of the overall crystal growth process [1, 2], but its meaning is not related to the conventional use of this term in chemical kinetics. It "has no fundamental significance and cannot give any indication of the number of elementary species involved in the growth process" [1]. It has been known from Volmer's work [3] that the temperature at which crystal growth takes place, i.e. the crystal interface temperature, is different from the bulk temperature. The heat transfer effects and the role of the thermal diffusion in crystal growth cannot be ignored [4, 5]. The driving force for the process, i.e. the supersaturation, is still being, however, calculated using solubility at bulk temperature. The main reason for this inconsistency is the difficulty to obtain the interface temperatures and concentrations.

It is generally accepted that there are two separate steps involved in the crystal growth process: diffusion followed by surface integration [2]. The driving force for each of these steps is expressed as a concentration difference i.e. for diffusion as $c_b - c_i$, where c_b is the bulk concentration and c_i -

Received: May 24, 2018; revised: November 19, 2018; accepted: January 11, 2019

To be cited as: Chem. Eng. Technol. 10.1002/ceat.201800255

Link to final VoR: https://doi.org/10.1002/ceat.201800255

the interfacial one, and for surface integration as $c_i - c^*_{T_b}$, where $c^*_{T_b}$ is the equilibrium solute concentration at the bulk solution temperature.

The existing mathematical models of crystal growth use empirical equations in the form $G = k_G \Delta c^g$ where *G* – crystal growth rate, k_G – conventional crystal growth proportionality constant, *g* – crystal growth power constant, Δc is the driving force, expressed as the concentration difference between the bulk concentration and the solubility of the solute at bulk temperature [2, 6-15]. The crystal growth rates estimated using empirical kinetic equations often lead to inconsistent results when different sources are used and compared [16-21] thus decreasing the confidence in their wider applicability and making models not transferable between crystallization processes and equipment.

Attempts to improve the crystal growth models have been made through introducing a temperature dependence of the kinetic constants [22-26], coupling mass transfer and a second order surface "reaction" [27], applying effectiveness factors of the crystal growth rate [4, 28], modelling solution-phase transitions using diffusion-limited kinetics [29]. The empirical character of the equations and thus their limited application, however, remained.

The aim of this paper is to calculate the driving force of crystallization in solution by modelling the simultaneous mass and heat transfer to and from the crystal interface and solving the challenging problem of diffusion with a moving interface. This problem has been solved analytically for uni-directional diffusion [30-32], but not for simultaneous uni- and bi-directional diffusion of mass and heat. A numerical solution has been applied in this work.

2. Modified diffusion-integration theory for crystal growth

The conventional way to calculate the driving force of crystallization Δc uses the difference between the bulk concentration c_b and the equilibrium concentration at the bulk temperature $c^*_{T_b}$

$$\Delta c = c_b - c^*_{T_b} \qquad (1)$$

The actual crystal growth, however, happens at the crystal interface where the concentration is the equilibrium one at T_i, not T_b:

$$\Delta c = c_b - c^*_{T_i} \qquad (2)$$

$c^*_{T_i}$ is the equilibrium concentration of the solute, based on the interface temperature T_i.

For positive solubility-temperature conditions, the conventional driving force is bigger than the actual one, i.e. this leads to an overestimation of the actual crystal growth rate.

In this work the interfacial crystallization parameters are calculated using the mass and energy balance equations for modelling the boundary layer phenomena. Solute molecules are attracted to the crystal interface due to the concentration difference between the bulk and the interface. They cross two solution zones before being integrated into the crystal, i.e. a molecular boundary layer and an integration layer (named here D-layer), in which desolvation takes place. Desolvation is the process of dissociation (separation) of the solute molecules from the solvent molecules surrounding them to integrate into the crystal, i.e. the solute molecules "desolvate". This causes a flux of solvent

molecules returning to the bulk through the boundary layer (backflow). The dominant mechanism of mass and heat transfer in the boundary layer is assumed to be diffusion. The mechanism of mass and heat transfer in the D-layer is unknown and is modelled as a pseudo-diffusion here. The following additional assumptions are applied:

1) Convection in the boundary layers is ignored. The critical Rayleigh number for a vertical plane indicating a transition from laminar to turbulent boundary layer and hence convective mass and heat transfer is orders of magnitude higher than the calculated value for the system (54655 for a boundary layer thickness of 0.0001 m).

2) Bulk concentration (c_b) and temperature (T_b) are constant. This may be justified for a small crystal in a large volume of the solution.

3) Molecular and thermal boundary layers may not be identical in space and time.

4) Crystal growth rate is size independent.

3. Mathematical formulation of mass and energy transfer through the desolvation and boundary layers and the crystal

The domain of consideration is the environment of a growing crystal in infinite bulk. Two phases are present – the crystal and the solution surrounding it. The crystallization of a single solute species is modelled.

For the one-dimensional case the changes of the concentration of solution c_l and the enthalpies of the solution ΔH_l and the crystal ΔH_c in the *x*-direction of crystal growth are represented by equations (3)-(5).

$$\frac{\partial(\rho_l c_l)}{\partial t} + D_m \frac{\partial^2(\rho_l c_l)}{\partial x^2} = 0 \qquad (3)$$

$$\frac{\partial(\rho_l C_l \Delta H_l)}{\partial t} + D_{hl} \frac{\partial^2(\rho_l C_l \Delta H_l)}{\partial x^2} = 0 \qquad (4)$$

$$\frac{\partial(\rho_c C_c \Delta H_c)}{\partial t} + D_{hc} \frac{\partial^2(\rho_c C_c \Delta H_c)}{\partial x^2} = 0 \qquad (5)$$

The index "*l*" denotes "liquid layer" and associates the corresponding parameter with its liquid layer value. Index "*b*" relates to the bulk liquid values of the parameters and index "*c*" – to the crystal". $\Delta H_l = \int_{T_{bulk}}^{T_i} C_{p_l} dT$ where C_{p_l} is the specific heat capacity of the solution. $\Delta H_c = \int_{T_{core}}^{T_i} C_{p_c} dT$, where C_{p_c} is the specific heat capacity of the crystal. The source terms have been ignored in the modelling equations due to the assumption of no overall change in mass and energy in the domain of consideration. Equations (3-5) represent the mass and energy transfer processes in the crystal and the boundary layer. The assumption of pure diffusion in the boundary layer simplifies the description of the process and the numerical solution of the mathematical model. The mass and heat transfer processes at the crystal interface could be influenced by more complex fluid dynamics phenomena e.g. double-diffusive convection [5] and solute redistribution in the vicinity of the interface and may require the inclusion of convective terms. Laminar boundary layers are simulated here.

Fig. 1 represents the main layers and parameters of the model. Two independent variables are considered, i.e. distance along X-axis, *x* and time, *t*. The co-ordinate system (X-axis) is fixed at the core of the crystal. At any time *t*, six layers are considered: in crystal - old layer and new layer; in liquid - molecular and thermal D- and boundary layers.

The D-point is defined as the boundary between the D-layer and the molecular boundary layer. The mechanism of the solute transport to the crystal interface changes at the D-point from diffusion in the boundary layer to pseudo-diffusion in the D-layer. The assumption for equilibrium at the crystal interface is a common one, although there is neither experimental nor theoretical proof of it.

The rate of crystal growth, *G*, can be expressed as

$$G = k_G\left(c_b - c_{T_i}^*\right) \tag{6}$$

This represents the driving force of a mass transfer process due to a concentration difference, where k_G is the mass transfer coefficient calculated as the ratio between the molecular diffusivity D_m and the thickness of the boundary layer δ_m [33].

The improved crystal growth model (equation 6) does still not allow for the presence of the D-layer. In this work, the driving force of crystallization is calculated as the difference between the concentration at the D-point, c_d and the concentration at the crystal interface, $c_{T_i}^*$

$$\Delta c = c_d - c_{T_i}^* \tag{7}$$

The growth rate G is calculated from the mass transfer equation

$$G = k_G^{'}\left(c_d - c_{T_i}^*\right) \tag{8}$$

where $k_G^{'}$ is the mass transfer coefficient based on the D-layer.

The product $G\rho_{cr}$ represents the mass flux into the crystal equal to the mass flux through the D-layer, i.e. $\frac{D_{m_{i-d}}}{\delta_{m_{i-d}}}\left(c_d - c_{T_i}^*\right)$, where $D_{m_{i-d}}$ is the apparent molecular diffusivity in the D-layer; $\delta_{m_{i-d}}$ is the thickness of the D-layer and their ratio i.e. $\frac{D_{m_{i-d}}}{\delta_{m_{i-d}}}$ represents the mass transfer coefficient, $k_G^{'}$.

Hence the mass balance at the interface can be represented by the relationship:

$$G\rho_{cr} = \frac{D_{m_{d-i}}\left(c_d - c_i\right)}{\delta_{m_{i-d}}} \tag{9}$$

The energy balance equation includes three heat fluxes at the crystal interface: heat effect of crystallization, Q_{cr}, heat flux to the crystal HF_c and heat flux to the liquid (D-layer), HF_l The highest temperature is that at the crystal interface, T_i. This temperature depends on the heat of crystallization, Q_{cr} and its dissipation into the crystal and the D-layer through the two heat fluxes, HF_c and HF_l .

The energy balance at the crystal interface is represented by

$$Q_{cr} = HF_c + HF_l \tag{10}$$

The two heat fluxes are expressed as diffusive fluxes, i.e.

$$HF_c = \frac{k_c}{\delta_c}\left(T_i - T_{i_p}\right), \quad (11)$$

where k_c is the thermal conductivity of the crystal; δ_c is the thickness of the new crystal layer at time *t*; T_{i_p} is the temperature at the old crystal interface.

$$HF_l = \frac{k_d}{\delta_{h_l}}\left(T_i - T_{i_d}\right), \quad (12)$$

where k_d is the apparent thermal conductivity of the D-layer; δ_{h_l} is the thickness of the thermal D-layer, T_{i_d} is the temperature at the D-point.

The heat of crystallization, Q_c can be calculated from *G* using the equation

$$Q_c = G\rho_c \Delta H_c \quad (13)$$

where ΔH_c is the enthalpy of crystallization.

The expression for the interface temperature is derived from the energy balance at the interface, i.e.

$$T_i = \frac{G\rho_c \Delta H_c + \frac{k_c}{\delta_{h_c}} T_{i_p} + \frac{k_d}{\delta_{h_l}} T_{i_d}}{\frac{k_c}{\delta_{h_c}} + \frac{k_d}{\delta_{h_l}}} \quad (14)$$

The model assumes that properties (conductivity, diffusivity, heat capacity) in the D-layer differ from the corresponding bulk properties.

Equations (3-5) can be simplified to represent the change of the concentration of the solute in the liquid, c_l, the temperature of the crystal, T_c , and the temperature of the liquid, T_l, along the *x*-coordinate and time:

$$\frac{\partial c_l}{\partial t} + D_m \frac{\partial^2 c_l}{\partial x^2} = 0 \quad (15)$$

$$\frac{\partial T_l}{\partial t} + D_{h_l} \frac{\partial^2 T_l}{\partial x^2} = 0 \quad (16)$$

$$\frac{\partial T_c}{\partial t} + D_{h_c} \frac{\partial^2 T_c}{\partial x^2} = 0 \quad (17)$$

The crystallization of potassium chloride from aqueous solution was simulated. The system was selected because data of the molecular and thermal diffusivities were available [34]. Although KCl is an ionic salt and exists as two separate ions (K^+ and Cl^-) in aqueous solutions, if the ions exist in pairs, a single molecular specie (KCl) can be assumed. Longsworth [34] gives a single value for each of the mass and thermal diffusivity of KCl.

4. Numerical solution of the crystal growth model

The model presented by equations (15-17) has been solved applying the Finite Difference Method with two discretization steps – along *x* (Δx) and along time (Δt). Crank-Nicholson discretisation scheme has been applied. The Fortran computer code for the numerical solution of the mathematical model uses Visual Studio 2012. The convergence of the numerical solution depends on the ratio $\Delta t/\Delta x$. The values of the numerical steps used are: Δt = 0.01 s , Δx = 0.0001 μm.

Relatively few complete sets of physico-chemical data for the solution properties are found in the literature, especially at high concentrations and for different temperatures. The data for potassium chloride are selected as representing one of the most complete sets, but even these require some extrapolation. Longsworth [34] quotes values for the thermal and mass diffusivities at concentrations up to a molality of 4. These data are extrapolated to a concentration of 0.4 *kg/kg* (equivalent to a molality of 5.3) as 1.7×10^{-7} $m^2.s^{-1}$ and 2.3×10^{-9} $m^2.s^{-1}$, respectively at 25 ℃. The diffusivities have been presented as functions of temperature and concentration. The data for the mass diffusivity are in good agreement with those quoted by Mullin [1]. The heat of crystallization is taken as minus the heat of solution [1], but this value is not quoted for a specific concentration of the solution and is at "room temperature". The solution heat capacity data [35] do not extend beyond a concentration of about 1 *M*. A constant value of 4000 $J.kg^{-1}.K^{-1}$ is assumed. The values given by Tanner and Lamb [36] are a little (<1%) higher at the higher concentrations. The density of the solid phase KCl is taken as 1980 $kg.m^{-3}$ [1]. The bulk concentration and temperature used in the model are 0.4 *kg KCl/kg water* and 25ºC. The solubility of potassium chloride is fitted in the linear form $c^*=0.002881 \times T + 0.28123$ using data from [37] over the range of interest. The thicknesses of the D-layers allowing a converged solution of the model equations are: molecular D-layer – 0.0008 μm; thermal – 0.0003 μm.

The simulation results are shown in Fig. 2-9. The changes of the growth rate (Fig. 2), concentrations at the interface and the D-point (Fig. 3), temperatures at the interface, D-point and crystal core (Fig. 4), the heat of crystallization, the heat flux to the crystal and the solution (Fig. 5) are plotted with respect to time. The profiles of the solute concentration in the liquid (Fig. 6), temperature in the crystal (Fig. 7) and temperature of the solution (Fig. 8) are shown with respect to distance perpendicular to the unit crystal area modelled. It is interesting to point out that the different parameters achieve steady state at different times: the growth rate *G* reaches steady state in approx. 230 *s* whereas the temperature of the crystal core does not reach steady state even in 400 *s*.

The growth rate, *G* and the solute concentration at the D-point, c_d follow similar profiles. This can be explained with the more significant changes in c_d compared to the changes in the solute concentration at the interface, $c^*_{T_i}$ and the mass transfer coefficient k'_G (equation 8).

Because of the higher thermal conductivity of the solid relative to the solution, initially more heat goes into the crystal (Fig. 5). However, as the crystal core temperature increases, the driving force decreases and the heat flux to the crystal decreases until it reaches an equilibrium stage when there is a balance between the two heat fluxes and they follow parallel paths at approximately half of the latent heat release.

The model assumes molecular and thermal pseudo diffusion in the desolvation layer. Stable numerical solutions are only achieved when these diffusion coefficients are orders of magnitude smaller than the normal diffusion coefficients of solute in an aqueous solution. This can be justified qualitatively by the large water flux away from the interface towards the bulk to achieve the desolvation.

The results demonstrate the interrelationship of the interface temperature and the concentration and their effect on the driving force for crystal growth. The solute is transferred from the bulk to the interface through the boundary layer that determines the resistance and thus the rate of the process.

The concentration and temperature profiles are close to linear that corresponds to the assumption of laminar boundary layers with mass and energy transfer by diffusion. The interface concentration is predicted as 0.3618 *kg KCl/kg water* and temperature as 28ºC. This concentration is calculated from the solubility of KCl at the interface temperature. Using the expression $\Delta c = c_b - c^*_{T_i}$, the driving force of crystallization (crystal growth) is found to be **0.0382** *kg KCl/kg water*

The solubility at the bulk temperature of 25 ºC is 0.3532 *kg KCl/kg water* and the driving force of crystallization calculated by the conventional method, i.e. $\Delta c = c_b - c^*_{T_b}$ is **0.0468** *kgKCl/kg water,* i.e. more than 20% **higher** than the one calculated at the predicted interface temperature.

The driving force of crystallization calculated using equation (7) (based on the D-layer) is even smaller i.e. 0.0018 *kg KCl/kg water* that can lead to the conclusion that the integration stage is the limiting one. The calculations apply to the steady state of the process. During the transient period the driving force calculated as the difference between the concentration at the D-point and the equilibrium concentration at the interface temperature, decreases from the initial maximum driving force for crystal growth to the steady state one (Fig. 3).

The crystal growth rate constant $k_G^{'} = \frac{D_m^{'}}{\delta_m}$ is determined as 961.7 $m.s^{-1}$.*[units for supersaturation]*$^{-1}$.

The pseudo molecular diffusivity is 0.577 x 10^{-12} $m^2.s^{-1}$ and thermal – 0.153 x10^{-12} $m^2.s^{-1}$. The steady state growth rate predicted considering both diffusion and integration steps was 1.17 x 10^{-6} $m.s^{-1}$. It is higher than the values shown by Sarig (0.1x10^{-6} $m.s^{-1}$ – 0.3x10^{-6} $m.s^{-1}$) [38] and Mullin (0.4x10^{-6} $m.s^{-1}$) [1], but the experiments have been run under desupersaturation conditions in the bulk (relative supersaturation 1.01), whereas constant bulk concentration is assumed in this study. It is also possible that the assumption of equilibrium at the crystal interface cannot be justified. The difference between the experimental and the predicted values for the growth rate *G* might also be due to the way of obtaining the cited growth rate values – direct measurements or through measurements of concentration, etc. The mathematical analysis performed in this work does not consider the effect of the crystal size on the crystal growth rate, i.e. it applies to size independent growth rate. Crystal growth dispersion [2, 39, 40] and its potential effect on the mass transfer is not considered in this model.

The experimental verification of the predicted concentration and temperature profiles is a challenge but attempts to monitor crystal interface parameters e.g. interface concentration [41] and temperature [42] have been made. Although applied in different areas of crystallisation, they can be used as a basis for developing a method to monitor concentration and temperature profiles around a growing crystal. Synchrotron light spectroscopy is another option.

The development of the boundary layers (molecular and thermal) are shown in Fig. 9. The simulation results show similar molecular and thermal boundary layer thicknesses during the transient period of the process and at the steady state. In reality, the molecular boundary layer limits the rate of the

solute supply to the growing surface depending on the mixing conditions in the crystallizer. Including mixing into the crystal growth model would improve its predictive capacity. The integration of the crystal growth model with molecular dynamics could be used to predict the growth of the different crystal faces and thus the crystal size and shape. These, however, are beyond the scope of the present work.

5. Conclusions

A new method of analysing crystal growth and its driving force in a system with two components – solute and solvent, has been proposed. The new model of crystal growth simulates the mass and energy transfer phenomena through the crystal and the solution. Mass and thermal diffusion through the desolvation and the boundary layers surrounding a growing crystal have been implemented. The transport of heat into and through the crystal required solution of the moving boundary diffusion problem.

The crystal growth rate, the solution concentration and temperature profiles and the crystal temperature profile have been predicted using basic physico-chemical properties of the system, i.e., molecular and thermal diffusivities, solubility, densities, specific heat and the heat of crystallization. The predicted interface properties fill in the current gap in the interface measurement techniques. The model has been verified using published *KCl* crystal growth data.

The driving force for crystal growth is calculated in three ways i.e. using equations (1), (2) and (7). The following values for the driving force have been obtained:

Equation (1), the conventional approach, using the difference between the bulk concentration and the equilibrium one calculated at the bulk temperature: 0.0468 *kg KCl/kg water.*

Equation (2), the modified approach using the difference between the bulk concentration and the equilibrium one calculated at the interface temperature: 0.0382 *kg KCl/kg water*.

Equation (7), the new approach calculating the driving force as the difference between the concentration at the D-point and the equilibrium concentration at the interface temperature: 0.0018 *kg KCl/kg water*.

The results show the overestimation of the driving force for crystal growth by the conventional approach by more than 20%.

Acknowledgements

The invaluable discussions with Dr G.E.Goltz and Prof. P.J. Heggs, University of Leeds, are gratefully acknowledged.

Symbols used

A_c	[m^2]	crystal area
c_l	[$kg.kg^{-1}$]	mass concentration of solute in solution (D-layer and boundary layer)
c_b	[$kg.kg^{-1}$]	mass concentration of solute in bulk
c_d	[$kg.kg^{-1}$]	mass concentration of solute at the D-point
c_i	[$kg.kg^{-1}$]	mass concentration of solute at interface
$c^*_{T_b}$	[$kg.kg^{-1}$]	equilibrium concentration of the crystallizing component based on bulk temperature
$c^*_{T_i}$	[$kg.kg^{-1}$]	equilibrium concentration of the crystallizing component based on the interface temperature
C_p	[$J.kg^{-1}.K^{-1}$]	specific heat capacity
D_m	[$m^2.s^{-1}$]	molecular diffusivity
D_h	[$m^2.s^{-1}$]	thermal diffusivity
G	[$m.s^{-1}$]	growth rate
g	[-]	crystal growth rate order ($G=k_G\Delta c^g$, $\Delta c=c-c^*$)
k_G	[$m.s^{-1}.unit\ concentration\ difference^{-g}$]	growth rate constant based on the concentration in bulk and the solubility at the interface temperature
k'_G	[$m.s^{-1}.unit\ concentration\ difference^{-1}$]	growth rate constant based on the concentration at the D-point and the solubility at the interface temperature
t	[s]	time
T	[ºC]	temperature
T_i	[ºC]	interface temperature
T_{i_o}	[ºC]	old interface temperature
T_{i_d}	[ºC]	temperature at the D-point
x		coordinate

Greek letters

ρ	[$kg.m^{-3}$]	density of phase (solution, solvent, crystal)
Δc	[$kg.kg^{-1}$]	concentration difference
ΔH	[J]	enthalpy change

Subscripts

b	bulk
c	crystal

i interface

l liquid

d D-point

m, h desolvation or boundary layer; *m* for molecular; *h* for thermal;

i-d desolvation layer (from interface (i) to D-point (d))

References:

[1] J. W. Mullin, Crystallization, 4th edition, Butterworth-Heinemann, Oxford **2001**.

[2] J. Garside, A. Mersmann, J. Nyvlt, Measurement of Crystal Growth Rates, European Federation of Chemical Engineering **1990**.

[3] M. Volmer, Kinetik der Phasenbildung, Dresden und Leipzig: Steinkopff **1939**.

[4] M. Matsuoka, J. Garside, *J. Cryst. Growth* **1993**, 129, 385—393.

[5] M. E. Thompson, J. Szekely, *J. Fluid Mech*. **1988**, 187, 409-433.

[6] A. Tadayon, , S. Rohani,, M.K. Bennett, M.K., *Ind. Eng. Chem. Res.* **2002**, 41, 6181-6193.

[7] W. Omar, J. Ulrich, *Cryst.Res.Technol.* **2003**, 38, 1, 31-34.

[8] P. Quintana-Hernandez, E. Bolanos-Reynoso, B. Miranda-Castro, L. Salcedo-Estrada, *AIChE J*. **2004**, 50, 7, 1407.

[9] Y. Bao, J. Zhang, Q. Yin, J. Wang, *J. Cryst. Growth* **2006**, 289,317-323.

[10] J. Scholl, D. Bonalumi, L. Vicum, M. Mazzotti, *Cryst. Growth Des.* **2006**, 4, 881.

[11] R.B.H. Tan, P.S. Chow, R.D. Braatz, *Cryst. Growth Des.* **2006**, 6, 1291.

[12] A. Borissova, G.E. Goltz, J. Kavanagh, T. Wilkins, *Med. Biol. Eng. Comput.*, **2010**, 48:649–659.

[13] Q. Su, Z. K. Nagy, C. D. Rielly, *Chem. Eng. Process.* **2015**, 89 41–53.

[14] S. K. Jha, S. Karthika, T.K. Radhakrishnan, *Resour.-Effic. Technol.* **2017**, 3, 94–100.

[15] M. Porru, L. Özkan, *Ind. Eng. Chem. Res.* **2017**, 56(34): 9578–9592.

[16] A. D. Randolph, M. A. Larson, Theory of Particulate Processes, Academic Press, New York/London **1971**.

[17] V. V. Kafarov, I. N. Dorohov, E. Koltzova, Systems Analysis of Chemical Technology Processes. Processes of Mass Crystallization from Solutions and Gas Phase, Nauka, Moscow **1983**.

[18] R. Zauner, A.G. Jones, *Chem. Eng. Sci*. **2000**, 55, 4219-4232.

[19] A. S. Bramley, M. J. Hounslow, R. L. Ryall, *Chem.Eng.Sci*. **1997**, 5, 747-757.

[20] R. Mohan, A. S. Myerson, *Chem. Eng. Sci*. **2002**, 57, 4277-4285.

[21] A. Borissova, *Chem. Eng. Process.: Process Intensif.* **2009**, 48, 268-278.

[22] G. Power, G. Hou, G., V. M. Kamaraju, G. Morris, Y. Zhao, B. Glennon, *Chem. Eng. Sci.* , **2015**, 133, 125–139.

[23] H. Li, Y. Kawajiri, M.A. Grover, R.W. Rousseau, DOI: 10.1021/acs.iecr.6b04914, *Ind. Eng. Chem. Res*. **2017**, 56, 4060−4073.

[24] H. Liu, P. Lan, S. Lu, S. Wu, *J. Cryst. Growth* **2018**, DOI: https://doi.org/10.1016/j.jcrysgro.2018.04.017

[25] P.M. Martins, F. Rocha, *Chem. Eng. Sci.* **2006**, 61, 5696 – 5703.

[26] T. Ogawa, *Prog. Crystal Growth and Charact*. *Mater.***1992**, 25, 51-101.

[27] S. K. Bermingham, PhD Thesis, Delft University Press, **2003**.

[28] J. Garside, N.S. Tavare, *Chem. Eng. Sci.***1981**, 36, 863-866.

[29] D.N. Petsev, K. Chen, O. Gliko, P.G. Vekilov, *PNAS* **2003**,100,792-796.

[30] P.V. Danckwerts, *Trans. Faraday Soc*. **1950**, 46, 701-712.

[31] J. Crank, The Mathematics of Diffusion, Clarendon Press, Oxford, **1956**.

[32] H.S. Carslaw, J.C. Jaeger, Conduction of Heat in Solids, 2nd edn., Clarendon Press, Oxford, **1959**.

[33] K.V. Kumar, *Ind. Eng. Chem. Res.* **2009**, 48, 11236–11240.

[34] L.G. Longsworth, *J. Phys. Chem.* **1957**, 61, 1557-1562.

[35] J.-L. Fortier, P.-A., Leduc J.E., Desnoyers, *J. Solution Chem.* **1974**, 3, 323-349.

[36] J. E. Tanner, F. W. Lamb, *J. Solution Chem*. **1978**, 7, 303-316.

[37] S. P. Pinho, E. A. Macedo, *J. Chem. Eng. Data* **2005**, 50, 29-32.

[38] S. Sarig, A. Glasner, J.A. Epstein N. Eidelman, *J. Cryst. Growth* **1977**, 39, 255-266.

[39] J. Ulrich, *Cryst. Res. Technol.* **1989**, 24, 249-257.

[40] J. Ulrich, M. Kruse, *Proc.11th Symp.Ind.Crys*.,Ed. A.Mersmann, **1990**.

[41] T. Egan, M. Rodriguez-Pascual, A. Lewis, *Chem.Eng.Technol*. **2014**, 37, 1283-1290

[42] L. W. Herron, C. G. Bergeron, *Phys. Chem. Glasses*, **1978**, 19, 89–94.

Figures:

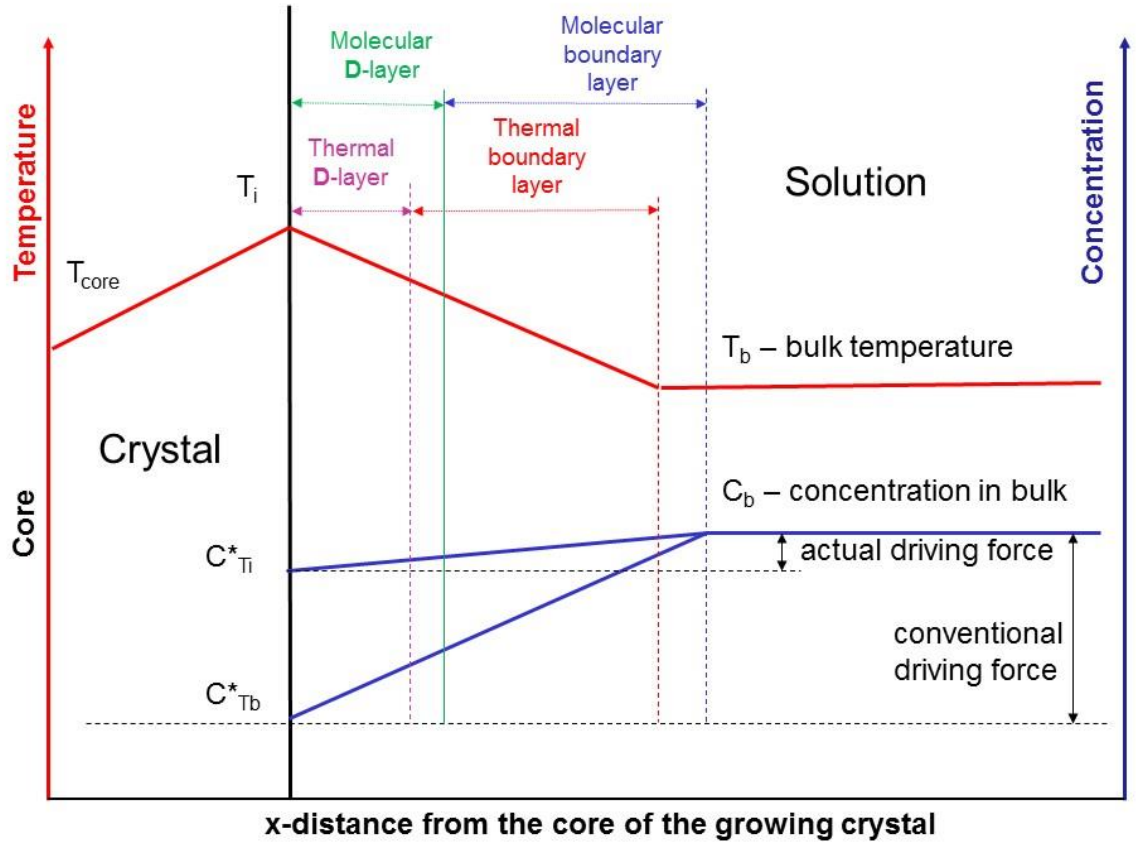

Figure 1 Conventional and real driving force of crystallization from solution (linearized profiles)

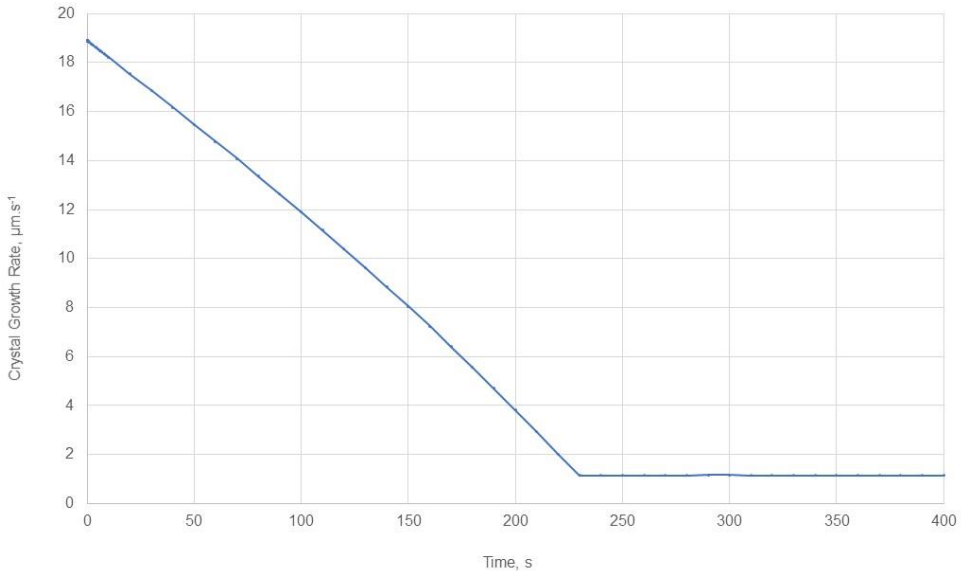

Figure 2 Temporal change of crystal growth rate of KCl in aqueous solution

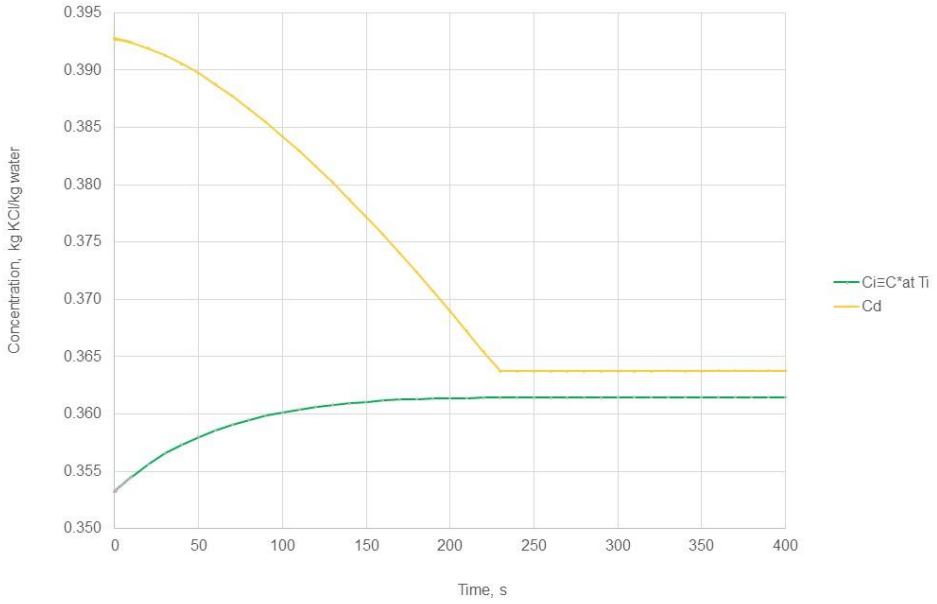

Figure 3 Temporal change of the concentration at the crystal interface and at the D-point

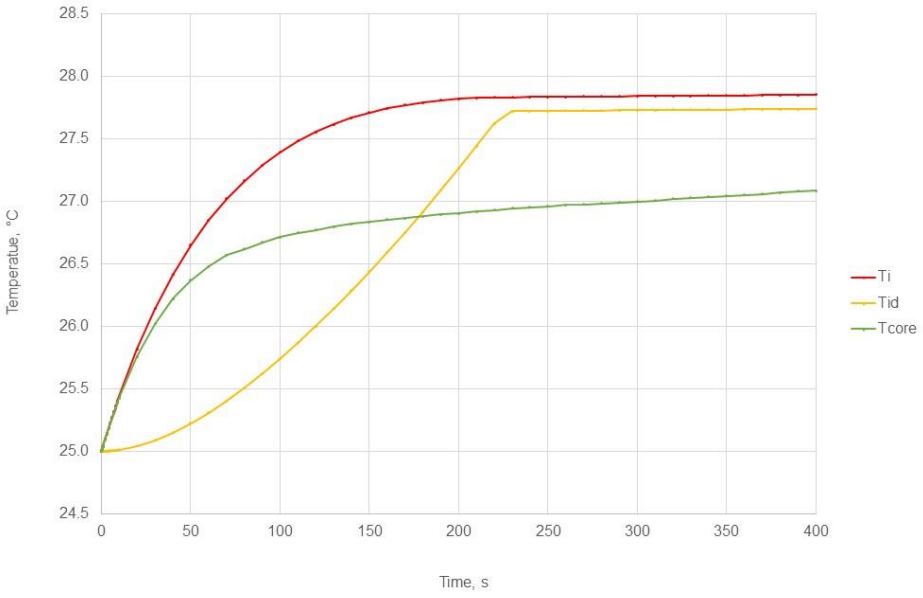

Figure 4 Temporal change of the temperature at the crystal interface, at the D-point and the crystal core

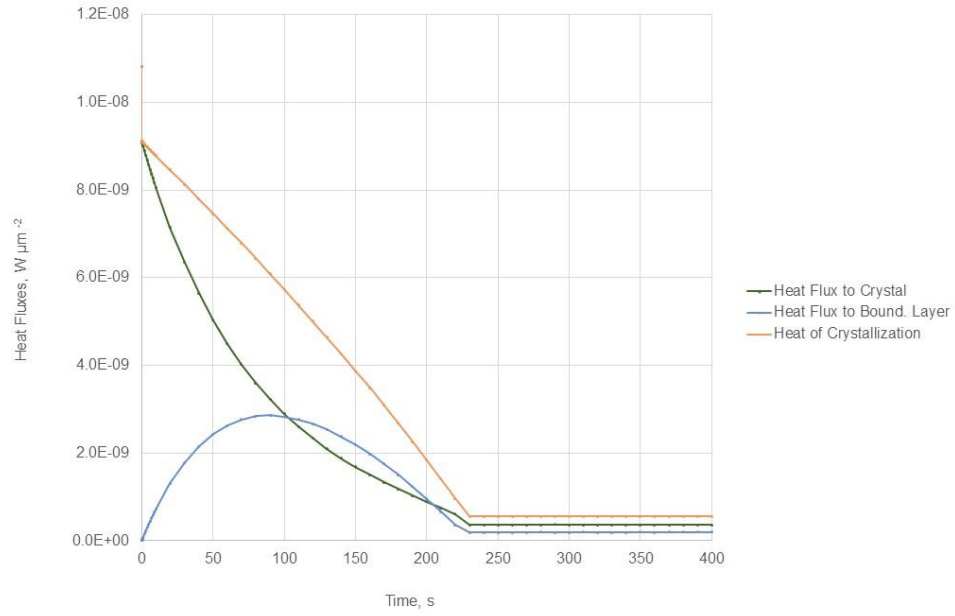

Figure 5 Temporal change of the heat fluxes to the crystal and the D-layer

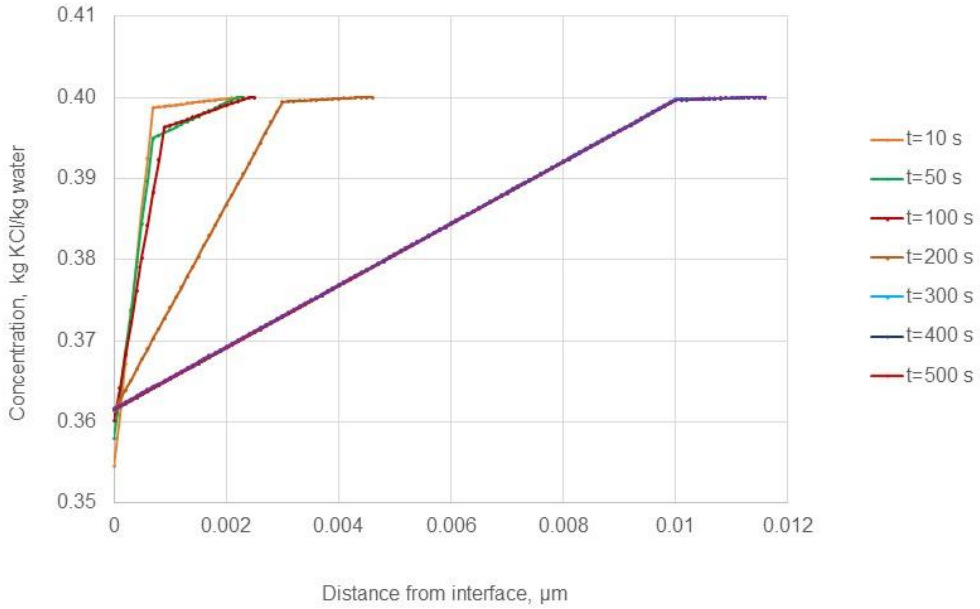

Figure 6 Concentration profiles in the D-layer and the boundary layer

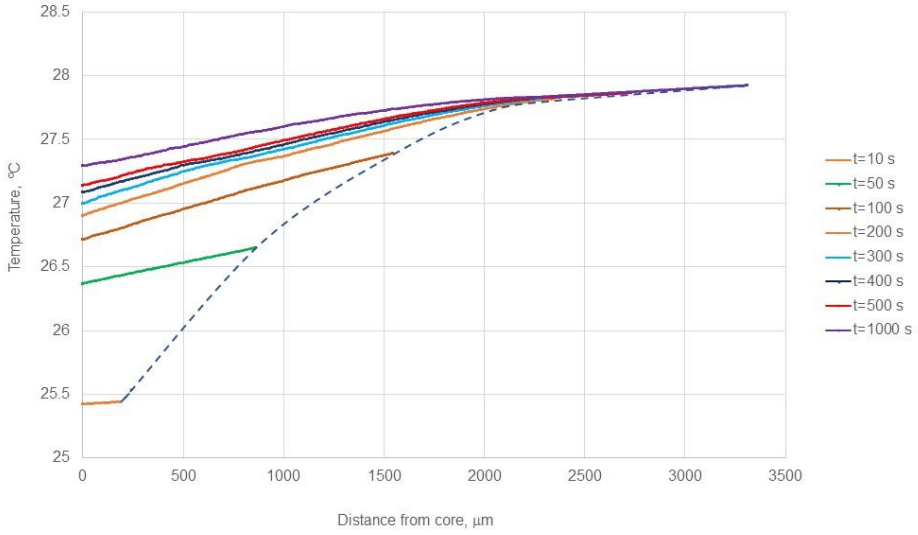

Figure 7 Temperature profiles in the crystal

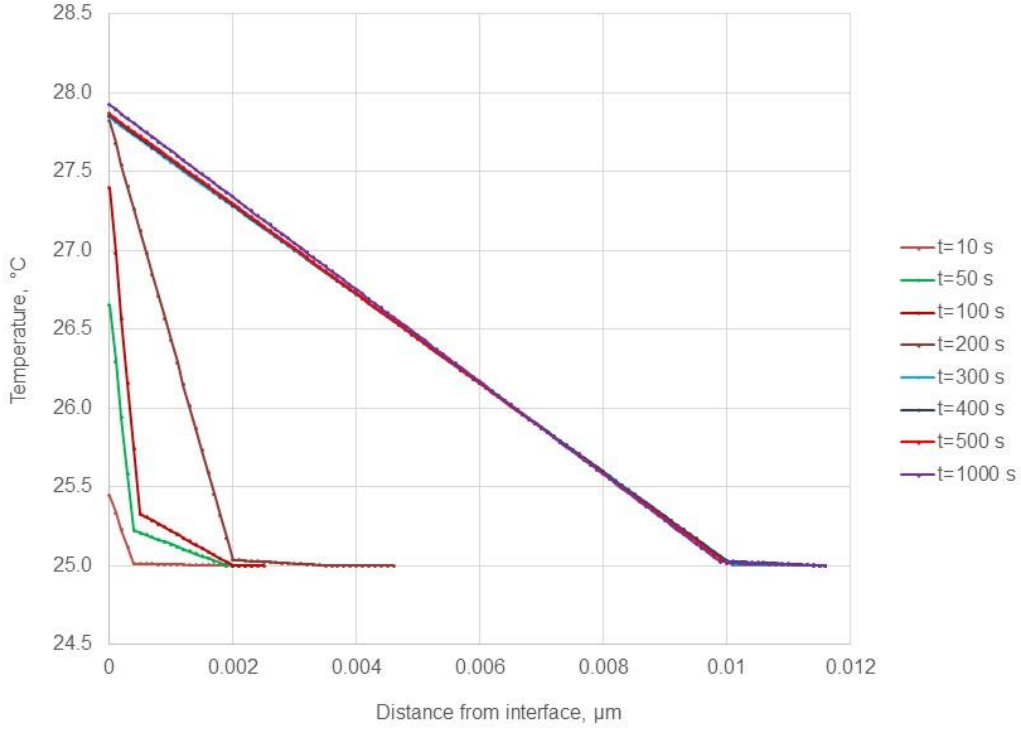

Figure 8 Temperature profiles in the solution

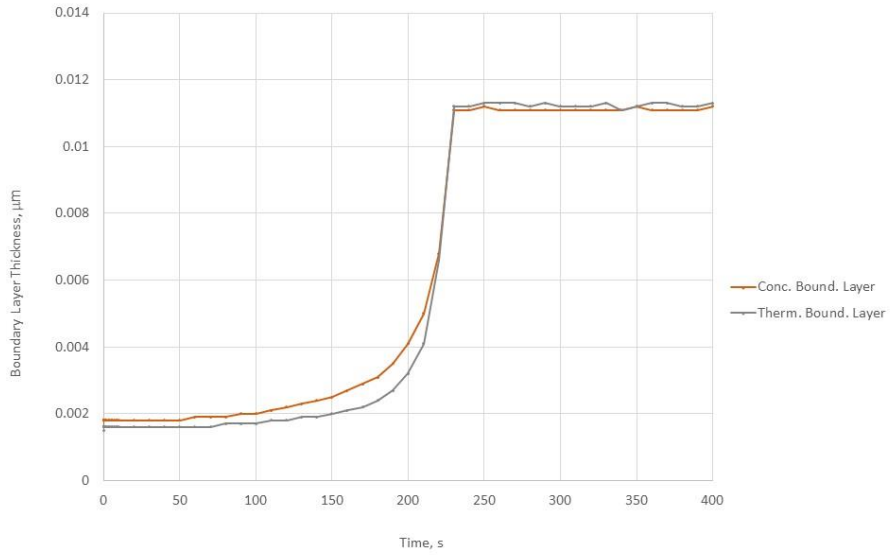

Figure 9. Development of the boundary layers